

PRIMAL: Power Inference using Machine Learning

Yuan Zhou^{*†}, Haoxing Ren[†], Yanqing Zhang[†], Ben Keller[†], Brucek Khailany[†], Zhiru Zhang^{*}

^{*}Cornell University [†]NVIDIA Corporation
{yz882, zhiruz}@cornell.edu {haoxingr, yanqingz, benk, bkhailany}@nvidia.com

Abstract

This paper introduces PRIMAL, a novel learning-based framework that enables fast and accurate power estimation for ASIC designs. PRIMAL trains machine learning (ML) models with design verification testbenches for characterizing the power of reusable circuit building blocks. The trained models can then be used to generate detailed power profiles of the same blocks under different workloads. We evaluate the performance of several established ML models on this task, including ridge regression, gradient tree boosting, multi-layer perceptron, and convolutional neural network (CNN). For average power estimation, ML-based techniques can achieve an average error of less than 1% across a diverse set of realistic benchmarks, outperforming a commercial RTL power estimation tool in both accuracy and speed (15x faster). For cycle-by-cycle power estimation, PRIMAL is on average 50x faster than a commercial gate-level power analysis tool, with an average error less than 5%. In particular, our CNN-based method achieves a 35x speed-up and an error of 5.2% for cycle-by-cycle power estimation of a RISC-V processor core. Furthermore, our case study on a NoC router shows that PRIMAL can achieve a small estimation error of 4.5% using cycle-approximate traces from SystemC simulation.

CCS Concepts

- Computing methodologies → Machine learning; Modeling methodologies;
- Hardware → Power estimation and optimization;

Keywords

Power estimation, machine learning

ACM Reference Format:

Yuan Zhou, Haoxing Ren, Yanqing Zhang, Ben Keller, Brucek Khailany, and Zhiru Zhang. 2019. PRIMAL: Power Inference using Machine Learning. In *The 56th Annual Design Automation Conference 2019 (DAC '19)*, June 2–6, 2019, Las Vegas, NV, USA. ACM, New York, NY, USA, 6 pages. <https://doi.org/10.1145/3316781.3317884>

1 Introduction

Modern VLSI design requires extensive optimization and exploration in a large design space to meet the ever-stringent requirements with respect to performance, area, and power. Existing ASIC CAD tools can provide reasonably accurate area and performance estimates at register transfer level (RTL) or even behavioral level with the aid of high-level synthesis (HLS) tools. However, in order

Permission to make digital or hard copies of all or part of this work for personal or classroom use is granted without fee provided that copies are not made or distributed for profit or commercial advantage and that copies bear this notice and the full citation on the first page. Copyrights for components of this work owned by others than ACM must be honored. Abstracting with credit is permitted. To copy otherwise, or republish, to post on servers or to redistribute to lists, requires prior specific permission and/or a fee. Request permissions from permissions@acm.org.

DAC '19, June 2–6, 2019, Las Vegas, NV, USA
© 2019 Association for Computing Machinery.
ACM ISBN 978-1-4503-6725-7/19/06...\$15.00
<https://doi.org/10.1145/3316781.3317884>

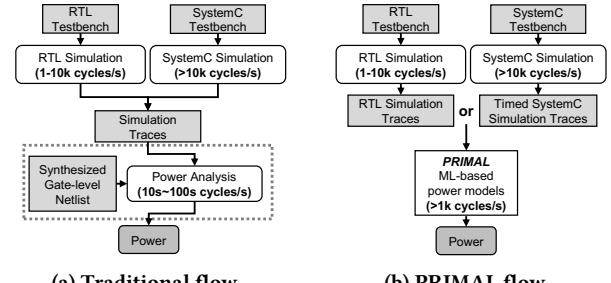


Figure 1: Conventional ASIC power estimation flow vs. PRIMAL – (a) With existing tools, designers must rely on slow gate-level power analysis for accurate power profiles. (b) PRIMAL trains ML-based power models for reusable IPs. Using the trained models, detailed power traces are obtained by running ML model inference on RTL or timed SystemC simulation traces.

to achieve power closure, designers must obtain detailed power profiles for a diverse range of workloads from different application use cases or even from different levels of design hierarchy. Currently, the common practice is to feed gate-level netlist and simulation results to power analysis tools such as Synopsys PrimeTime PX (PTPX) to generate cycle-level power traces. Figure 1a depicts a typical ASIC power analysis flow, which offers accurate estimates but runs at a very low speed (in the order of 10-100s of cycles per second). Given the high complexity of present-day ASIC designs, it can take hours or days to perform gate-level power analysis for one intellectual property (IP) core under desired workloads.

An alternative is to analyze power above gate level. There exists a rich body of research on power analysis at RTL or a higher abstraction level [3, 4, 6, 7, 14, 20, 21, 23, 24]. These efforts typically make use of measured constants or simple curve fitting techniques such as linear regression to characterize the power of a given circuit, improving the speed of power analysis at the expense of estimation accuracy. For accurate power characterization, many low-level details of the circuit need to be modeled, including standard cell parameters, sizing of the gates, and clock gating status of the registers. Gate-level power analysis uses them to estimate the switching capacitance and activity factor of each circuit node. However, these low-level details are unavailable at (or above) RTL by design. It is also very difficult for simple analytical models or linear regression models to capture the complex nonlinear relationship between the register toggles and the total switching capacitance.

To enable fast and accurate high-level power estimation, we propose PRIMAL¹, a learning-based power inference framework that enables fast and accurate power characterization of reusable IP cores at RTL or behavioral level. PRIMAL leverages gate-level power analysis to train machine learning (ML) models on a subset of verification testbenches. These trained models can then be

¹PRIMAL stands for power inference using machine learning.

used to infer power profiles of the same IP core under different user-specified workloads. Figure 1b illustrates the inference flow of PRIMAL, which only requires inputs from RTL or SystemC simulation to rapidly generate accurate power estimates (>1k cycles per second). By greatly reducing the required number of gate-level simulation cycles, PRIMAL allows designers to perform power-directed design space exploration in a much more productive manner. The major technical contributions of this work are fivefold:

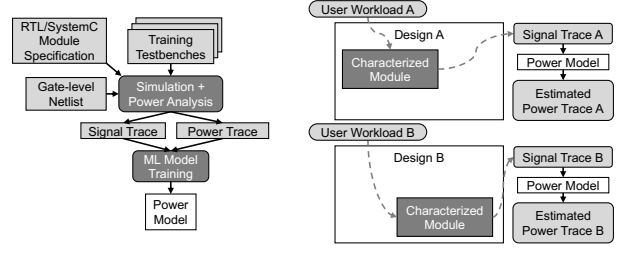
- We present PRIMAL, a novel ML-based methodology for rapid power estimation with RTL or timed SystemC simulation traces. The trained ML models can provide accurate, cycle-by-cycle power inference for user workloads even when they differ significantly from those used for training.
- We investigate several established ML models for power estimation, and report trade-offs between accuracy, training effort, and inference speed. Our study suggests that nonlinear models, especially convolutional neural nets (CNNs), can effectively learn power-related design characteristics for large circuits.
- We explore feature engineering techniques to construct image representations from register traces. The constructed features are used by CNNs for training and inference.
- We demonstrate that PRIMAL is at least 50x faster on average than PTPX for cycle-accurate power estimation with a small error. Notably, our CNN-based approach is 35x faster than PTPX with a 5.2% error for estimating power of a RISC-V core. PRIMAL also achieves a 15x speedup over a commercial RTL power analysis tool for average power estimation.
- Using a NoC router design as a case study, we demonstrate that PRIMAL can be extended to enable accurate power estimation for timed SystemC design.

The remainder of this paper is organized as follows: Section 2 surveys related work, and Section 3 presents the overall design methodology and intended use cases of PRIMAL. Section 4 introduces our feature construction methods. Experimental results are reported in Section 5. Section 6 gives concluding remarks.

2 Related Work

Power estimation is an extensively studied research topic. Existing works focus on power estimation from behavioral-level and RTL. Behavioral-level power estimation provides optimization guidance early in the design flow. In an earlier work, Chen et al. [7] combine profiling and simple analytical models to estimate FPGA power consumption. Later efforts use the HLS tool to perform scheduling and back-annotation, and rely on RTL power analysis [3], gate-level power analysis [21], or a per-control-step ML power model [14] for power estimation.

Compared to behavioral-level analysis, more implementation details are available at RTL. Earlier works in RTL power estimation use simple regression models, such as linear regression and regression trees, to characterize small circuit blocks [4, 6, 20]. The regression models are trained with gate-level power analysis results. Average power and cycle-by-cycle power of the whole design can be obtained by summing up the outputs from multiple models. PrEsto [23] uses linear models to characterize larger modules, where heavy feature engineering and feature selection are applied to reduce the complexity of power models. A more recent work by Yang et al. [24] uses a single linear model to characterize the whole design. A feature selection technique based on singular value decomposition (SVD) is applied to reduce model complexity so that the regression model can be efficiently mapped onto an FPGA. Both PrEsto and [24] can provide cycle-by-cycle power estimates.



(a) Characterization phase (b) Estimation phase

Figure 2: Two phases of the PRIMAL work flow — Power models are trained **once per module**, then used across different workloads and in different designs that instantiate the module.

In general, existing RTL power estimation techniques either model small circuit sub-modules or try to use simple regression models to characterize the whole design. Sub-module-level modeling cannot accurately reflect the power consumption of intermediate logic, and simple regression models such as linear models are not a good fit for large, complex designs.

3 PRIMAL Methodology

Unlike previous works, PRIMAL uses state-of-the-art ML models for fast and accurate high-level power estimation. Our methodology can readily be applied to RTL and SystemC power estimation. Figure 2 shows the two phases of the PRIMAL work flow. The characterization phase (Figure 2a) requires an RTL/SystemC model of the module, the gate-level netlist, and a set of unit-level testbenches for training. RTL or SystemC simulation traces and the power traces generated by gate-level power analysis are used to train the ML models. The characterization process only needs to be performed once per IP block. The trained power models can then be used to estimate power for different workloads as illustrated in Figure 2b.

It is important to note that the training testbenches may be very different from the actual user workloads. For example, designers can use functional verification testbenches to train the power models, which then generalize to realistic workloads. By using state-of-the-art ML models, PRIMAL can accommodate diverse workloads and model large, complex circuit blocks. The ML models are trained for cycle-by-cycle power estimation to provide detailed power profile and enable more effective design optimization.

In this work we explore a set of established ML models for power estimation. The classical ridge linear regression model is used as a baseline. We also experiment with gradient tree boosting, a promising non-linear regression technique [17]. For linear models and gradient tree boosting models, we apply principal component analysis (PCA) [12] to the input data to reduce model complexity and avoid overfitting. We also study the efficacy of deep learning models, which are capable of approximating more complex non-linear functions. Specifically, we experiment with multi-layer perceptron (MLP) and CNN models for power estimation. MLP contains only fully-connected network layers and is more compute-efficient than CNN. However, the parameter count of MLP grows quickly with respect to the feature size of the design, resulting in overfitting and training convergence issues. CNNs have shown impressive performance in image classification tasks. Since the power of a certain logic cone is only correlated with a small set of registers, the convolutional windows of CNNs are able to gather useful information if the input images are constructed properly. In addition, thanks to the structure of convolutional layers, CNN is a more scalable choice than MLP for large designs since the parameter count of a CNN does not increase significantly as the input image size grows.

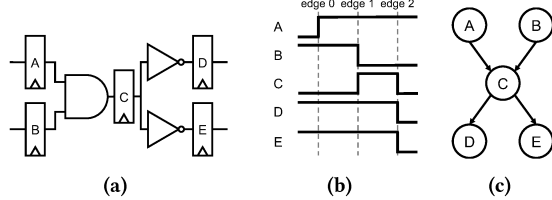


Figure 3: Simple circuit example with waveform of register outputs and register connection graph.

	A	B	C	D	E
edge 0	1	0	0	0	0
edge 1	0	1	1	0	0
edge 2	0	0	1	1	1

	Reg-to-pixel mapping	channel 0: non-switching	channel 1: 0→1	channel 2: 1→0																																				
edge 1	<table border="1"> <tr><td>A</td><td>B</td><td>C</td></tr> <tr><td>D</td><td>E</td><td>d</td></tr> <tr><td>d</td><td>d</td><td>d</td></tr> </table>	A	B	C	D	E	d	d	d	d	<table border="1"> <tr><td>1</td><td>0</td><td>0</td></tr> <tr><td>1</td><td>1</td><td>0</td></tr> <tr><td>0</td><td>0</td><td>0</td></tr> </table>	1	0	0	1	1	0	0	0	0	<table border="1"> <tr><td>0</td><td>0</td><td>1</td></tr> <tr><td>0</td><td>0</td><td>0</td></tr> <tr><td>0</td><td>0</td><td>0</td></tr> </table>	0	0	1	0	0	0	0	0	0	<table border="1"> <tr><td>0</td><td>1</td><td>0</td></tr> <tr><td>0</td><td>0</td><td>0</td></tr> <tr><td>0</td><td>0</td><td>0</td></tr> </table>	0	1	0	0	0	0	0	0	0
A	B	C																																						
D	E	d																																						
d	d	d																																						
1	0	0																																						
1	1	0																																						
0	0	0																																						
0	0	1																																						
0	0	0																																						
0	0	0																																						
0	1	0																																						
0	0	0																																						
0	0	0																																						

Figure 4: Basic feature encoding methods – (a) 1D switching encoding. (b) Default 2D encoding for edge 1 in Figure 3b.

4 Feature Construction

This section describes the feature construction procedure using the circuit in Figure 3a as an example. Figure 3b shows the register waveform, where each “edge” in the figure corresponds to a clock rising edge. We use register switching activities in the simulation traces as input features, because register switching activities are representative of the circuit’s state transitions. In addition, there is a one-to-one correspondence between registers in RTL and gate-level netlist². Because we use cycle-accurate power traces from gate-level simulation as ground truth, the ML models are essentially learning the complex relationship between the switching power for all gate-level cells and register switching activities. For clarity we focus on RTL power estimation in this section, but our feature construction methods can also be naturally applied or extended to SystemC power estimation.

Feature Encoding for Cycle-by-Cycle Power Estimation – For cycle-by-cycle power estimation, we use RTL register and I/O signal switching activities as input features without any manual feature selection. Switching activities of both internal registers and I/O signals are required to capture complete circuit state transitions. These features can be easily collected from RTL simulation. Because we are targeting cycle-by-cycle power estimation, each cycle in the simulation trace is constructed as an independent sample.

A good feature encoding should differentiate between switching and non-switching events. A concise encoding, which we refer to as *switching encoding*, is to represent each register switching event as a 1, and non-switching event as a 0. For an RTL module with n registers, each cycle in the RTL simulation trace is represented as a $1 \times n$ vector. Figure 4a shows the corresponding encoding for the waveform in Figure 3b. Each vector in Figure 4a represents one cycle (one clock rising edge to be precise) in the waveform. We use this one-dimensional (1D) switching encoding for all but the CNN models. The same feature encoding is used in [24].

In order to leverage well-studied two-dimensional (2D) CNN models, we create a three-channel 2D image representation for every cycle in the register trace. For an RTL module with n registers,

²In cases where retiming with register optimization is used, mapping between RTL and gate-level registers can be retrieved from the logic synthesis tool.

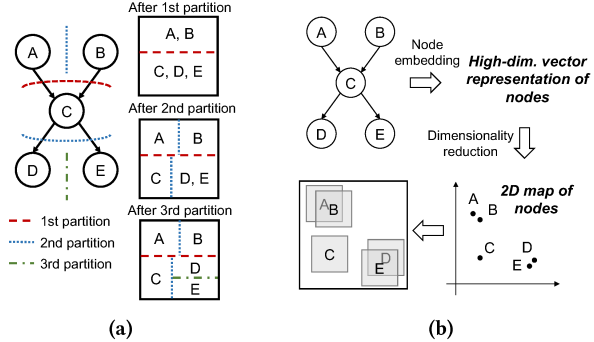


Figure 5: Graph-based register mapping schemes – (a) Register mapping based on graph partitioning. The register connection graph is recursively partitioned into two parts. Each partition also divides the map into two non-overlapping parts. (b) Register mapping based on node embedding. Node embedding maps each graph node as a point in high-dimensional space, then dimensionality reduction techniques project the high-dimensional representations onto the 2D space. In the generated mapping each register occupies a unit square whose area is equivalent to one pixel.

we use a $\lceil \sqrt{n} \rceil \times \lceil \sqrt{n} \rceil \times 3$ image to encode one cycle in the RTL simulation trace. We use one-hot encoding in the channel dimension to represent the switching activities of each register: non-switching is represented as $[1, 0, 0]$, switching from zero to one is represented as $[0, 1, 0]$, and switching from one to zero is $[0, 0, 1]$. We refer to this encoding as *default 2D encoding*. Figure 4b shows how we encode edge 1 of the waveform in Figure 3b. If the total number of pixels in the image is greater than n , we add padding pixels to the image, shown as d ’s in Figure 4b. These padding pixels do not represent any register in the module, and they have zero values in all three channels in our implementation. Every other pixel corresponds to one register in the module. For this default 2D encoding, the registers are mapped by their sequence in the training traces. For example, since in Figure 3b the order of registers is A, B, C, D , and E , in each channel the top-left pixel in Figure 4b corresponds to A , the top-right pixel is mapped to C , and the center pixel refers to E . We observe that this default mapping from registers to pixels is not completely random. The tool flow we are using would actually cluster most of the registers within a submodule together. As a result, in our experiments, this default 2D encoding actually preserves a considerable amount of circuit structural information.

Mapping Registers and Signals to Pixels – In the default 2D encoding described above, the mapping between registers and pixel locations are determined by the way the registers are arranged in the trace file. The amount of structural information that is preserved is dependent on the tool flow. As a result, this mapping method cannot guarantee meaningful local structures in the constructed images. Registers that are mapped to adjacent pixels may not be correlated or physically connected. CNNs are most effective when there are spatial relationships in their 2D inputs. Therefore, the register-to-pixel mapping should reflect the connectivity or physical placement of the registers. Since the gate-level netlist of the design is available during the characterization phase, it is possible to use the outputs of logic synthesis tools to map RTL registers to netlist nodes. Because we only use register and I/O switching activities, we ignore all combinational components and only extract register connection graphs when processing the gate-level netlist. The graph for the example circuit in Figure 3a is shown in Figure 3c. Each node

Table 1: Benchmark information — We evaluate PRIMAL with a diverse set of benchmark designs. For NoC router and RISC-V core, the test sets are realistic workloads which are potentially different from the corresponding training set.

Design	Description	Register + I/O signal count	Gate count	PTPX throughput (cycles/s)	Training set (# cycles)	Test set (# cycles)
qadd_pipe	32-bit fixed point adder	160	838	1250	Random stimulus (480k)	Random stimulus (120k)
qmult_pipe{1, 2, 3}	32-bit fixed point multiplier with 1, 2, or 3 pipeline stages	{384, 405, 438}	{1721, 1718, 1749}	{144.9, 135.1, 156.3}	Random stimulus (480k)	Random stimulus (120k)
float_adder	32-bit floating point adder	381	1239	714.3	Random stimulus (480k)	Random stimulus (120k)
float_mult	32-bit floating point multiplier	372	2274	454.5	Random stimulus (480k)	Random stimulus (120k)
NoCRouter	Network-on-chip router for a CNN accelerator	5651	15076	44.7	Unit-level testbenches (910k)	Convolution tests (244k)
RISC-V Core	RISC-V Rocket Core (SmallCore)	24531	80206	45	RISC-V ISA tests (2.2M)	RISC-V benchmarks (1.7M)

Table 2: Training time of different ML models

Design	PCA	Ridge Regression	XGBoost	MLP	CNN
arithmetic units	~10 min	~1 min	~15 min	~25 min	~3 h
NoCRouter	~7 h	~15 min	~1 h	~1.5 h	~10 h
RISC-V Core	~20 h	~30 min	~1.5 h	~7 h*	~20 h*

* Use random 50% training data per training epoch.

in the graph corresponds to one register in the design, and two nodes are connected if their corresponding registers are connected by some combinational data path.

We propose two graph-based methods for generating register-to-pixel mappings, which introduce local structures into the images according to the structural similarities between nodes. Notice that the proposed graph-based mapping methods only change the register mapping in the width and height dimensions of the image: we still use the channel-wise one-hot encoding for every register. Each register's contribution to each pixel is proportional to the overlapping area of the register's occupied region and the pixel. In other words, with the graph-based encoding methods the pixel values are non-negative real numbers rather than binary numbers.

The first method is based on graph partitioning, in which the graph is recursively divided into two partitions of similar sizes, and the partitions are mapped to corresponding regions in the image (see Figure 5a). The area allocated for each partition is computed according to the number of nodes in the partition. The second method is based on node embedding. Node embedding techniques map each node in the graph to a point in a vector space, where similar nodes are mapped close to each other in the vector space. Our flow for embedding-based register mapping is shown in Figure 5b. We use *node2vec* [10] for node embedding, then apply PCA [12] and t-SNE [16] to project the vector representations to 2D space. The resulting 2D vector representations are scaled according to the image size and indicate the mapping locations of the registers.

5 Experiments

We have implemented our proposed framework in Python 3.6, leveraging *networkx* [11], *metis* [13], and a *node2vec* package [10]. MLP and CNN models are implemented using *Keras* [2]. Other ML models are realized in *scikit-learn* [19] and *XGBoost* [8]. We conduct our experiments on a server with an Intel Xeon E5-2630 v4 CPU and a 128GB RAM. We run neural network training and inference on a NVIDIA 1080Ti GPU. The SystemC models of our designs are synthesized with Mentor Catapult HLS. We use Synopsys Design Compiler for RTL and logic synthesis, targeting a 16nm FinFET standard cell library. The RTL register traces and gate-level power traces are obtained from Synopsys VCS and PTPX, respectively. Gate-level power analysis is performed on another server with an Intel Xeon CPU and 64GB RAM using a maximum of 30 threads.

5.1 Benchmarks

Table 1 lists the benchmarks used to evaluate PRIMAL. Our benchmarks include a number of fixed- and floating-point arithmetic units from [18]. We also test our approach against two complex designs — a NoC router used in a CNN accelerator and a RISC-V processor core. The NoC router block is written in SystemC and synthesized to RTL by an HLS tool. The RISC-V core is an RV64IMAC implementation of the open-source Rocket Chip Generator [5] similar to the SmallCore instance. We use different portions of random stimulus traces as training and test sets for the arithmetic units. For the NoC router and the RISC-V core, we select functional verification testbenches for training and use realistic workloads for test. For the NoC router, we test on actual traces of mesh network traffic from a CNN accelerator SoC. In the RISC-V experiment, *dhystone*, *median*, *multiply*, *qsort*, *towers*, and *vvadd* form the set of test workloads.

5.2 RTL Power Estimation Results

Figure 6 summarizes the results for RTL power estimation. Here we use RTL register traces as the raw input and apply the feature construction techniques described in Section 4. Two percent of the training data is used as a validation set for hyper-parameter tuning of the ML models. They are also used for early stopping when training the deep neural networks.

All models except CNNs use the 1D switching encoding, while CNNs use the 2D image encoding methods introduced in Section 4. We also experimented with 1D one-hot encoding, where we encode the switching activity of each register using three binary numbers as described in Section 4. Since the results with such encoding is similar with 1D switching encoding, we omit the results due to space limitations. For ridge regression and gradient tree boosting, we apply PCA to reduce the size of input features to 256, except for *qadd_pipe* which has only 160 features with 1D feature encoding. We use three-layer MLP models for the arithmetic unit and four-layer MLP models for the NoC router and the RISC-V core. We use an open-source implementation [1] of ShuffleNet V2 [15] for CNN-based power estimation because of its parameter-efficient architecture and fast inference speed. The *v0.5* configuration in [15] is used for the arithmetic units, while the *v1.5* configuration is used for the NoC router and RISC-V core. The CNN models are trained from scratch. *CNN-default*, *CNN-partition*, and *CNN-embedding* in Figure 6 refer to the default 2D encoding, graph-partition-based register mapping, and node-embedding-based register mapping methods introduced in Section 4, respectively.

Cycle-by-Cycle Power Estimation Results — We use normalized root-mean-squared-error (NRMSE) as our evaluation metric. Suppose the ground-truth power trace is represented as a n -dimensional vector \mathbf{y} , and the estimated power trace is a vector $\hat{\mathbf{y}}$

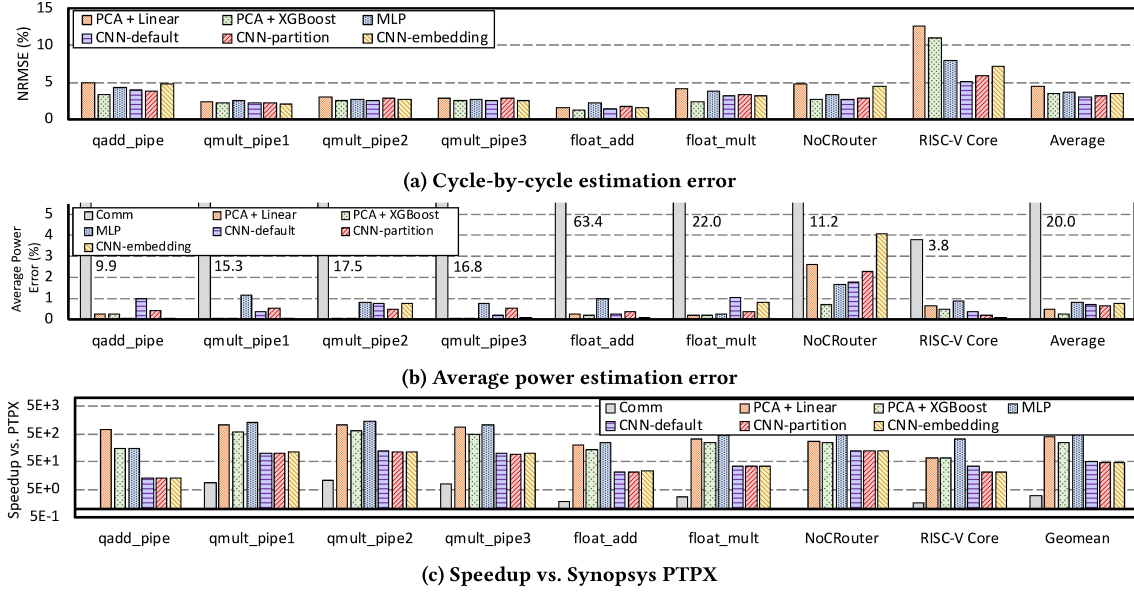


Figure 6: Performance of different machine learning models on test sets — The ML models used by PRIMAL achieve high accuracy for both cycle-by-cycle and average power estimation, while offering significant speedup against both Synopsys PTPX and the commercial RTL power analysis tool (Comm). PRIMAL is also significantly more accurate than Comm in average power estimation.

of the same shape. Then

$$NRMSE = \frac{1}{\bar{y}} \sqrt{\frac{\sum_{i=1}^n (\mathbf{y}_i - \hat{\mathbf{y}}_i)^2}{n}}$$

As shown in Figure 6a, all ML models can achieve an average estimation error of less than 5% across our benchmarks. The training time for each ML model is summarized in Table 2. For small designs, XGBoost offers competitive accuracy with much less training effort. CNN models show significant advantage over other ML models for larger designs like the RISC-V core. Notably, our CNN model with default 2D encoding achieves an impressive 5.2% error on the test set, while MLP, XGBoost and Linear model achieves around 8%, 11% and 13% error, respectively. Noticeably, the estimation error for the RISC-V core is considerably higher than other designs. Compared with other benchmarks, the RISC-V core contains $\sim 5x$ to $\sim 95x$ more gates but has only five pipeline stages. Each pipeline stage is significantly more complex and harder to model. In addition, it is harder to create a comprehensive training set for the models to approximate a larger design.

Figure 7 compares the estimation of CNN-default and PCA+Linear with the ground truth power trace. The CNN estimation fits the ground truth curve more closely. These results demonstrate the superior capability of deep neural networks in approximating complex non-linear functions. We observe that the graph-based register mapping methods do not provide much benefit over default 2D encoding because of the rich structural information in the default encoding. In fact, the advanced encodings result in a lower accuracy on some benchmarks. One possible reason is that with the graph-based encoding methods, information of multiple registers is clustered onto a small number of pixels, making it more difficult for the CNN models to distinguish between high-power and low-power samples. Essentially, with the 2D encoding methods, we are trying to figure out the latent space of toggling registers and show it in

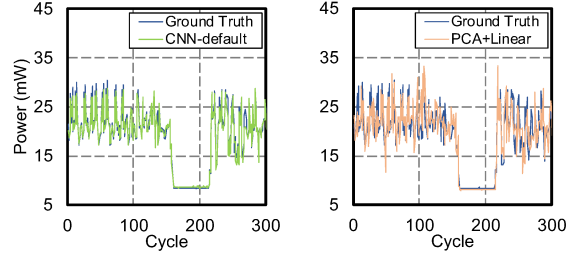


Figure 7: Ground truth vs. CNN-default and PCA+Linear for RISC-V — Showing 300 cycles from the dhystone benchmark. the two-dimensional space. This problem itself is an interesting research direction, and we leave it for future work.

Average Power Estimation Results — The average power consumption for a workload can be easily obtained from a cycle-accurate power trace. We compare the ML-based techniques with a commercial RTL power analysis tool (Comm). According to Figure 6b, all of the ML techniques achieve less than 1% average error, while the commercial tool has an average error of 20%. NoCRouter has higher error for average power estimation, because the training set and the test set have very different average power. Interestingly, while the CNN models achieve similar or higher accuracy compared with other ML models for cycle-by-cycle power estimation, their accuracy for average power estimation is slightly worse because the CNN models tend to consistently overestimate or underestimate power by a very small margin. This behavior may be caused by a mismatch in average power between the training and test sets: the CNN models learn the average power of the training set better, causing a small yet consistent shift in their estimations for the test set. The ML models require a significant amount of time to be trained for complex designs as shown in Table 2. Therefore, the commercial RTL power analysis tool is still favorable for power estimation of non-reusable modules.

Speedup — Figure 6c presents the speedup of the commercial RTL power analysis tool and the PRIMAL techniques against Synopsys

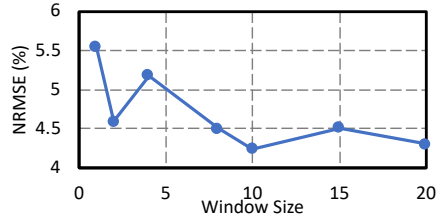


Figure 8: SystemC power estimation accuracy of NoC Router vs. window size, using a VGG16 CNN model.

PTPX. Notice that for PRIMAL, the reported speedup is for model inference only, which is the typical use case. While the commercial tool is only ~ 3 x faster than PTPX on average, all ML models achieve much higher estimation speed. Even the most compute-intensive CNN models provide ~ 50 x average speedup against PTPX. Linear model, XGBoost and MLP has an additional 8x, 5x and 10x speedup compared with CNNs, respectively. Note that the linear and gradient tree boosting models are executed on CPU, while MLP and CNN inference is performed on a single GPU. As a result, if more efficient implementations of the ML models and more compute resources are available, higher speedup can be expected with a modest hardware cost. For small designs, linear model and gradient tree boosting are almost always more favorable choices, since the neural network models do not provide significant accuracy improvement but require much more compute and training effort. For complex designs such as the RISC-V core, CNN provides the best accuracy with ~ 35 x speedup, while other models are faster but less accurate.

5.3 NoC Router SystemC Power Estimation

We use the NoC router design as a case study to demonstrate the applicability of PRIMAL to SystemC power estimation. We continue to employ functional verification testbenches as our training set, and test on 3.5k cycles of chip-level convolution testbenches. Cycle-by-cycle power estimation may not be applicable to SystemC designs, because traces that consist of the values of SystemC variables over time are transaction-accurate rather than cycle-accurate. For our specific NoC router design, a SystemC variable trace can differ from the RTL trace by up to seven cycles. Therefore, aside from cycle-by-cycle power estimation, we also train the ML models to estimate the average power inside fixed-size time windows. In such cases, we perform an element-wise sum of the encoded features inside the time window and use the results for ML model training and inference. While the SystemC and RTL trace lengths are the same for our training and test sets, this may not be generally true: the effect of SystemC trace inaccuracy is sometimes accumulative, resulting in significant differences in the lengths of SystemC and RTL simulation traces. Our feature preprocessing technique does not address this issue, and we leave the question of how to handle trace length mismatch for future work.

Because SystemC power estimation is more difficult with the non-constant signal shift, we fine-tune a VGG16 model [22] pre-trained on ImageNet [9] for window-by-window estimation. Compared with the ShuffleNet V2 models, VGG16 has more parameters and larger receptive fields in its convolutional layers, enabling it to model even more complex functions. The estimation accuracy of the VGG16 model with different window sizes is shown in Figure 8. The default 2D encoding is used for this experiment. While the CNN model performs reasonably well for small window sizes, there is a clear error decrease when the window size is larger than seven as the effect of trace inaccuracy is mitigated. When the window size is larger than 8, the CNN model is able to achieve less than 4.5%

error, which is satisfactory in most cases. Nevertheless, the error of SystemC power estimation remains higher than that of RTL power estimation because of the trace inaccuracy and the information loss in the feature construction process.

6 Conclusions

We have presented PRIMAL, a learning-based framework that enables fast and accurate power estimation for ASIC designs. Using state-of-the-art ML models, PRIMAL can be applied to complex hardware such as a RISC-V core, and the trained power models can generalize to workloads that are dissimilar to the training testbenches. The ML-based techniques achieve less than 5% and 1% average error for cycle-by-cycle and average power estimation, respectively. Compared with Synopsys PTPX, PRIMAL provides at least 50x speedup across our selection of benchmarks. We also demonstrate that PRIMAL can be readily extended to SystemC power estimation through a case study on NoC router.

Acknowledgements

This research was supported in part by NSF Award #1512937 and the Intel ISRA Program. We thank the anonymous reviewers for providing suggestions and helpful feedback to our work.

References

- [1] Keras Implementation of ShuffleNet V2. <https://github.com/opconty/keras-shufflenetV2>, 2018.
- [2] Keras: The Python Deep Learning library. <https://keras.io/>, 2018.
- [3] S. Ahuja et al. Power Estimation Methodology for A High-Level Synthesis Framework. *International Symposium on Quality of Electronic Design*, 2009.
- [4] J. H. Anderson and F. N. Najm. Power Estimation Techniques for FPGAs. *Transactions on VLSI Systems*, 2004.
- [5] K. Asanović et al. The Rocket Chip Generator. Technical Report UCB/EECS-2016-17, Department of Electrical Engineering and Computer Sciences, University of California, Berkeley, 4 2016.
- [6] A. Bogliolo et al. Regression-Based RTL Power Modeling. *Transactions on Design Automation of Electronic Systems*, 2000.
- [7] D. Chen et al. High-Level Power Estimation and Low-Power Design Space Exploration for FPGAs. *Asia and South Pacific Design Automation Conference*, 2007.
- [8] T. Chen and C. Guestrin. XGBoost: A Scalable Tree Boosting System. *Proc. International Conference on Knowledge Discovery and Data Mining*, 2016.
- [9] J. Deng et al. Imagenet: A Large-Scale Hierarchical Image Database. *Conference on Computer Vision and Pattern Recognition*, 2009.
- [10] A. Grover and J. Leskovec. node2vec: Scalable Feature Learning for Networks. *International Conference on Knowledge Discovery and Data Mining*, 2016.
- [11] A. Hagberg et al. Exploring Network Structure, Dynamics, and Function using NetworkX. Technical report, Los Alamos National Lab.(LANL), Los Alamos, NM (United States), 2008.
- [12] I. Jolliffe. Principal Component Analysis. In *International Encyclopedia of Statistical Science*. Springer, 2011.
- [13] G. Karypis and V. Kumar. A Fast and High Quality Multilevel Scheme for Partitioning Irregular Graphs. *Journal on Scientific Computing*, 1998.
- [14] D. Lee et al. Dynamic Power and Performance Back-Annotation for Fast and Accurate Functional Hardware Simulation. *Design, Automation & Test in Europe*, 2015.
- [15] N. Ma et al. Shufflenet v2: Practical Guidelines for Efficient CNN Architecture Design. *arXiv preprint arXiv:1807.11164*, 2018.
- [16] L. v. d. Maaten and G. Hinton. Visualizing Data using t-SNE. *Journal of Machine Learning Research*, 2008.
- [17] L. Mason et al. Boosting Algorithms as Gradient Descent. *Proc. Advances in Neural Information Processing Systems*, 2000.
- [18] OpenCores.org. Fixed Point Math Library for Verilog :: Manual. https://opencores.org/project/verilog_fixed_point_math_library/manual, 2018.
- [19] F. Pedregosa et al. Scikit-Learn: Machine Learning in Python. *Journal of Machine Learning Research*, 2011.
- [20] S. o. Ravi. Efficient RTL Power Estimation for Large Designs. *International Conference on VLSI Design*, 2003.
- [21] Y. S. Shao et al. Aladdin: A Pre-RTL, Power-Performance Accelerator Simulator Enabling Large Design Space Exploration of Customized Architectures. *ACM SIGARCH Computer Architecture News*, 2014.
- [22] K. Simonyan and A. Zisserman. Very Deep Convolutional Networks for Large-Scale Image Recognition. *arXiv preprint arXiv:1409.1556*, 2014.
- [23] D. Sunwoo et al. PrEsto: An FPGA-Accelerated Power Estimation Methodology for Complex Systems. *International Conference on Field Programmable Logic and Applications*, 2010.
- [24] J. Yang et al. Early Stage Real-Time SoC Power Estimation using RTL Instrumentation. *Asia and South Pacific Design Automation Conference*, 2015.